Check for updates

# Distribution and off−shelf transport of dissolved manganese in the East China Sea

Zhaowei Wang[1], Jingling Ren[2,3]*, Jiliang Xuan[4], Sumei Liu[2] and Jing Zhang[5]

[1]College of Environmental Science and Engineering, Dalian Maritime University, Dalian, China, [2]Frontiers Science Center for Deep Ocean Multispheres and Earth System, and Key Laboratory of Marine Chemistry Theory and Technology, Ministry of Education, Ocean University of China, Qingdao, China, [3]Laboratory for Marine Ecology and Environmental Science, Qingdao National Laboratory for Marine Science and Technology, Qingdao, China, [4]State Key Laboratory of Satellite Ocean Environment Dynamics, Second Institute of Oceanography, Ministry of Natural Resources, Hangzhou, China, [5]State Key Laboratory of Estuarine and Coastal Research, East China Normal University, Shanghai, China

To gain a better understanding of the geochemical behavior of dissolved manganese (Mn) in the marginal seas with respect to distribution and exchange fluxes, more than 200 water samples were collected in the East China Sea (ECS) in May, August, and October of 2013. The concentration of dissolved Mn in the ECS ranged from 1.1 to 81.5 nM, with a gradual decrease with distance from the shore. Seasonal distribution of dissolved Mn varies significantly in the Changjiang estuary, mainly regulated by freshwater input from the Changjiang (Yangtze River) and redox variations. The ECS continental shelf is an important source of Mn for adjacent waters, and the export of Mn−rich coastal waters had an important effect on its re-distribution and internal cycling. The dynamic variation fluxes of water and dissolved Mn across the 100− and 200−m isobaths in the ECS were calculated with an aid of the Finite−Volume Coastal Ocean Model (FVCOM). The ECS continental shelf exported $(5.69 \pm 1.14) \times 10^8$ mol/yr of Mn into the East/Japan Sea from the Tsushima Strait. The Kuroshio surface waters receive an additional $(1.02 \pm 3.12) \times 10^8$ mol/yr of Mn from the ECS continental shelf through a cross−shelf exchange process, which could potentially affect dissolved Mn in the Northwest Pacific. Our data suggest that off-shelf transport from the ECS continental shelf is essential for understanding the biogeochemical cycles of trace metals in the Northwest Pacific Ocean and the East/Japan Sea.

KEYWORDS

dissolved manganese, transport, flux, East China Sea, redox

## 1 Introduction

Manganese (Mn) is an important tracer in the transport of terrestrial materials, yet it exists at micromolar levels in the ocean. Considerable data regarding the distribution of dissolved Mn has been obtained during the last 40 years, including in the Pacific Ocean (Landing and Bruland, 1987; Resing et al., 2015; Zheng et al., 2019), Indian Ocean (Saager

et al., 1989)), Southern Ocean (Middag et al., 2011), Atlantic Ocean (Shiller, 1997; Wu et al., 2014; Middag et al., 2015), and Arctic Ocean (Colombo et al., 2020). Its distribution reflects external sources, scavenging removal away from these sources, as well as internal cycling in the ocean (Van Hulten et al., 2016). External sources, such as riverine input and eolian dust, are responsible for elevated concentrations of dissolved Mn in coastal waters and the surface layer (Sim and Orians, 2019). Mn can also enter the water column by reductive dissolution from anoxic or suboxic sediments (Heiser et al., 2001), lateral transportation from marginal sediments, or hydrothermal input (Middag et al., 2011). However, most of the existing Mn data comes from studies conducted in open waters and knowledge on the internal cycling and transport from marginal seas remains limited. Understanding the processes controlling the distribution of dissolved Mn in the marginal seas is therefore important for studying the cycle of trace metals in the ocean.

Marginal seas are located between continents and open oceans. Concentrations of dissolved Mn typically increase in marginal seas where waters receive abundant continental materials from rivers and coastlines (Aguilar-Islas and Bruland, 2006; Roy et al., 2013). The East China Sea (ECS) is one of important marginal seas in the North Pacific and has the largest continental shelf (Sherman and Tang, 1999). It is connected to the mainland China and linked with the Yellow Sea and the South China Sea. The Changjiang (Yangtze River) flows into the ECS from mainland China, forming an enormous plume of freshwater into the ECS ($10^{12}$ m$^3$/yr, Zhang et al., 2007). The western boundary current (Kuroshio Waters, KW) flows along the ECS shelf edge, playing an important role in the exchange of material and heat energy in the China marginal seas (Guo et al., 2012). The ECS continental shelf has complex circulation systems under the effect of monsoons and is simultaneously influenced by both fluvial input and the Kuroshio incursion. The exchange between the ECS and the KW is an important process controlling the geochemical cycle of biogenic elements (Liu, 2000; Wang et al., 2021; Zhang et al., 2021a), which has received increased attention in the past decade. Therefore, a better understanding of the transport processes in the present study is important to the overall knowledge of marine biogeochemical cycles of Mn in the ECS.

On-shelf and off-shelf transport are crucial for marine processes, which have generated interest involving the geochemical budgets of biogenic elements (Ren et al., 2015; Ding et al., 2019; Zhang et al., 2021b). In this study, we examined the distribution and seasonal variations of dissolved Mn across the ECS from the eutrophic coastal waters to the oligotrophic KW. By using numerical simulations and tracer experiments, we calculated the dynamic exchange flux of dissolved Mn across the 100– and 200–m isobaths in the ECS to improve our understanding of the impact of off-shelf transport of terrestrial materials from the ECS to the western Pacific.

# 2 Materials and methods

## 2.1 Field sampling

Seawater samples from the ECS were collected at different seasons in 2013 from the *R/V* "Dongfanghong 2" (August 2013) and the *R/V* "Bei Dou" (May 2013 and October 2013) (Figure 1A). Restricted by

ship time and logistical problems, a limited number of stations were monitored in May 2013 and October 2013. A CTD-rosette assembly with Niskin bottles (Model: Sea-Bird 911$^{plus}$) was used to measure the profiles of temperature, salinity, and dissolved oxygen (DO) in the water column at grid stations. The internal black rubber springs and "O" rings were replaced by silicon springs and silicon "O" rings. The silicon springs and silicon "O" rings were strictly cleaned with Milli-Q water before the cruise. All Niskin bottles were thoroughly cleaned by soaking in diluted acid (0.1 M HCl) at least one week, then filled with Milli-Q water and sealed by plastic bags before sampling. We conducted inter–calibration of different water sampling systems (MITLESS from MIT, newly designed X–Vane, and the Niskin bottle) during the August cruise of 2013 to insure the quality of our sampling data. MITLESS samplers were demonstrated as suitable for trace metal sampling (Zhang et al., 2015). Considering we found no significant differences between final Mn concentrations using MITLESS and Niskin bottle, we consider our sampling using Niskin bottle free from contamination and adapted for trace metal sampling in the ECS continental shelf (Zhang et al., 2015). After collection, all samples were filtered through pre-cleaned Whatman polycarbonate filters (pore size: 0.4 µm) in a class-100 clean bench. Prior to use, the filters were immersed in an ultrapure HCl solution (pH = 2; Merck) for 24 h and then rinsed with Milli–Q water until a neutral pH was obtained. The filtrates were kept in 250 mL LDPE bottles (Nalgene), double-bagged in zipper-seal polyethylene bags, and stored at –18°C until analyzed in the laboratory. Blanks were prepared at sea by filtering a known volume of Milli-Q water with methods identical to the bulk sample sets. The amount of suspended particulate matter (SPM) was measured by determining the weight of particles retained on the filters. During the summer cruise, additional samples were collected at 0.5m depth for dMn concentrations using a modified "towed fish" to characterize dissolved Mn in the inner Changjiang Estuary. Those samples were pumped into the laboratory clean unit on the ship through Teflon-lined plastic tubing using a pneumatic diaphragm pump.

## 2.2 Analytical methods

Dissolved Mn samples were analyzed in the lab after the cruise by using the flow injection analysis method developed by Aguilar-Islas and Bruland (2006). Briefly, this is a sensitive flow injection analysis method based on spectrophotometric determination from the reaction between leucomalachite green and sodium periodate using nitrilotriacetic acid as an activator. One minor modification of our system is that we changed the buffer solution in-line before column loading with ammonium acetate buffer instead of borate buffer. The procedural blanks, detection limits and precisions of the above-described method are shown in Supplementary Material. The total procedural blank in this study was 0.95 ± 0.07 nM, and the detection limit was 0.21 nM. As an independent comparison, the certification samples collected from the North Atlantic GEOTRACES reference samples as of 2008 (GS) and the certified reference material NASS-6 (National Research Council, Canada) were analyzed for dissolved Mn. The results of our group were consistent with the consensus values and those of other laboratories (all differences were within 10%).
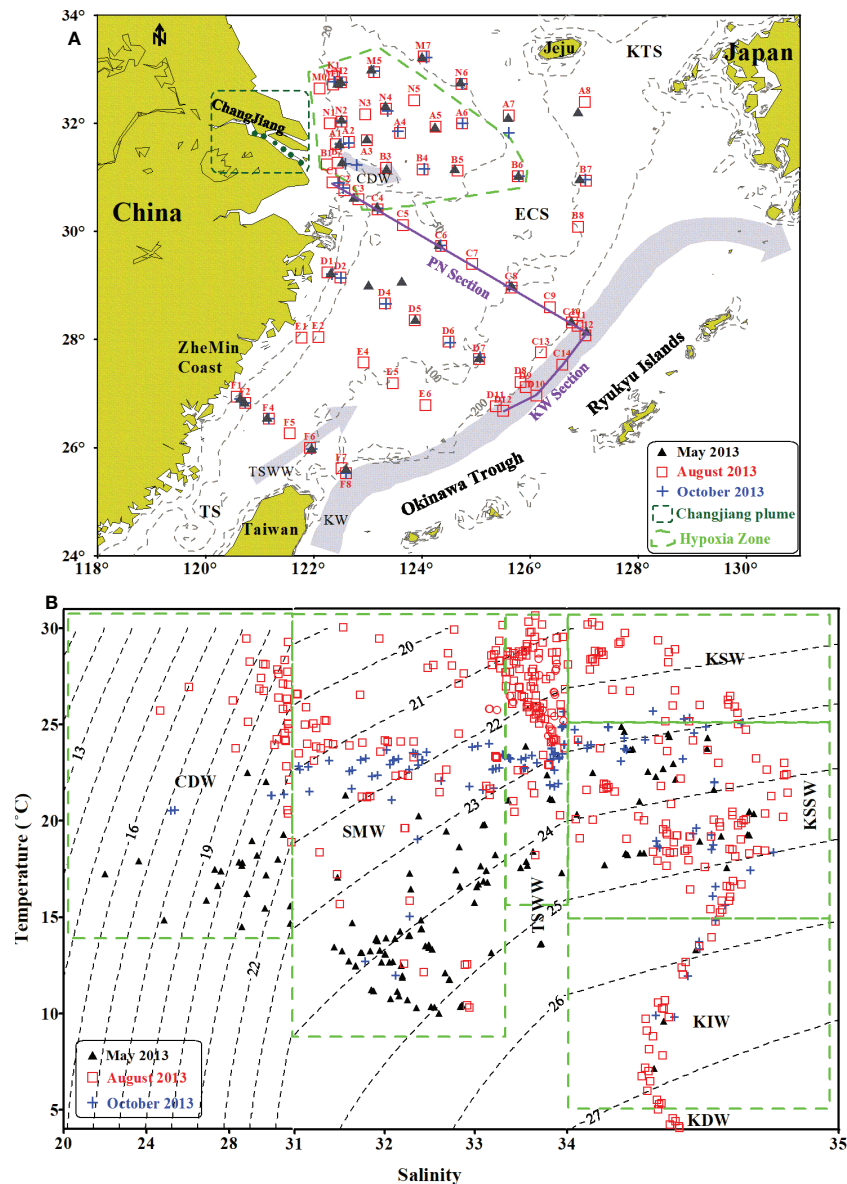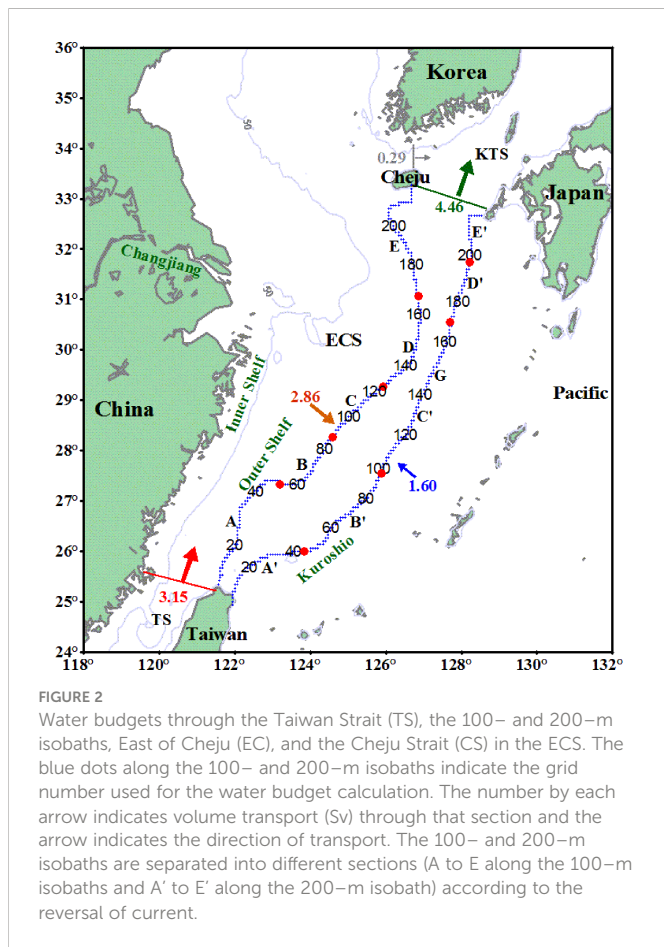
**FIGURE 1**

**(A)** Sampling stations of three cruises across the East China Sea in 2013 (▲: May, □: August, +: October), with illustrations of circulation regimes, including the Changjiang Diluted Water (CDW), Kuroshio Water (KW) and Taiwan Strait Warm Water (TSWW). Sampling stations in the Changjiang plume are indicated with a rectangle. The PN Section (from the Changjiang Estuary to the Ryukyu Islands) and KW Section (along the KW in the ECS edge) are highlighted by purple solid lines. The green dashed area represents the Hypoxia Zone that occurred in near-bottom waters outside the Changjiang Estuary (DO < 100 μM) in summer 2013. **(B)** A plot of salinity-temperature data for the ECS, which includes the Changjiang Diluted Water (CDW), Shelf Mixed Water (SMW), Taiwan Strait Warm Water (TSWW), Kuroshio Surface Water (KSW), Kuroshio Subsurface Water (KSSW), Kuroshio Intermediate Water (KIW), and Kuroshio Deep Water (KDW) (Su, 1998; Qi et al., 2014). (ECS, East China Sea; TS, Taiwan Strait; KTS, Korea/Tsushima Strait).

## 2.3 Numerical simulations

The Finite–Volume Coastal Ocean Model (FVCOM) with a large domain of Bohai Sea, Yellow Sea, ECS and part of the Pacific Ocean was used for a high-resolution (10 km) simulation of the currents in the ECS. Detailed information including bathymetric, driving forces, boundary conditions, and model results can be found in (Xuan et al., 2016; Xuan et al., 2017; Xuan et al., 2019) and Wang et al. (2021). The 100–m isobath was usually chosen as the cut-offs to study the contribution of ECS continental shelf transport, while the 200–m isobath was a reference line where Kuroshio flows along with it (Guo et al., 2006). Therefore, the Taiwan Strait (TS), 100– and 200–m

isobaths, sections of East of Cheju (EC) and the Cheju Strait (CS) were selected as the exchange boundaries to calculate the water budgets across the ECS (Figure 2). The off–shelf transport flux of dissolved Mn across the 100–m isobath was assumed to be the total Mn export from the ECS continental shelf, then the transport flux on the 200–m isobath enters into the Kuroshio current. The volume transport and water mass balance in the ECS were compared with published results to validate the simulation results (Xuan et al., 2019). To improve our understanding of the on–shelf and off-shelf transport of dissolved Mn across the ECS continental shelf, we focused on the current velocities and flow directions on the 100– and 200–m isobaths in the ECS at each grid points. The grid points of the 100– and 200–m isobaths

**FIGURE 2**
Water budgets through the Taiwan Strait (TS), the 100− and 200−m isobaths, East of Cheju (EC), and the Cheju Strait (CS) in the ECS. The blue dots along the 100− and 200−m isobaths indicate the grid number used for the water budget calculation. The number by each arrow indicates volume transport (Sv) through that section and the arrow indicates the direction of transport. The 100− and 200−m isobaths are separated into different sections (A to E along the 100−m isobaths and A′ to E′ along the 200−m isobath) according to the reversal of current.

generally follow their water depths. A depth–stretched coordinate system was used to specify 40 vertical layers with a vertical resolution of approximately 1–5 m in the mixed layer (Wang et al., 2021).

# 3 Results

## 3.1 Hydrographic setting of the study area

Basic hydrographic regimes in the ECS can be identified based on the characteristics of potential temperature and salinity (Figure 1B), including 1) Changjiang Diluted Water (CDW); 2) Taiwan Strait Warm Water (TSWW); 3) Kuroshio Waters (KW, including Kuroshio Surface Water [KSW], Kuroshio Subsurface Water [KSSW] and Kuroshio Intermediate Water [KIW]) and 4) Shelf Mixed Water (SMW). The distributions of temperature, salinity, SPM, and DO in the surface and bottom waters of the ECS are shown in Figures 3–5. Lower salinity (S < 31) was associated with higher SPM, indicating the influence of CDW in the coastal area of Changjiang Estuary. In spring and summer, the Changjiang plume extended predominantly toward the east and northeast (the direction from the Changjiang mouth to Jeju Island), while the trend of CDW spreading southward was strengthened in autumn. Characterized by a high temperature and high salinity (T > 22°C, S > 33), the TSWW reflects the northward movement of warm water off the Min-Zhe coasts of China. It occurs in the middle of the ECS continental shelf at depths of 50–100 m. With the aid of southwest monsoons, the TSWW

becomes more obvious in summer (Jan et al., 2002). Upwelling conditions are sustained by the incursion of the KW on the outer shelf area of the ECS where the highest salinity (> 34) and lowest SPM concentrations occurred. The nearshore KW branch current in the ECS is impeded by the enhanced CDW during the summer. A water mass with salinity lower than 33 is defined as Shelf Mixed Water (SMW), which is a mixture of CDW, TSWW, and KW. Remarkably, a hypoxic zone (DO < 3 mg/L) occurs in near-bottom waters of the Changjiang Estuary in summer.

## 3.2 Distributions of dissolved Mn across the ECS and seasonal variations

Distributions of dissolved Mn in the ECS in spring, summer, and autumn are depicted in Figures 3–5. The distribution of dissolved Mn in the ECS showed a trend of gradually decreasing from the nearshore to the sea, reflecting impacts from terrestrial input. The intrusion of the KW with relatively low dissolved Mn concentrations resulted in low concentrations of dissolved Mn occurring along the ECS shelf edge. Concentrations of dissolved Mn in the ECS ranged from 2.5 to 29.1 nM in spring (7.0 ± 4.1 nM, n=138), 1.1 to 81.5 nM in summer (13.2 ± 15.4 nM nM, n=349), and 1.1 to 15.2 nM in autumn (5.0 ± 2.3 nM, n=133) in 2013. Higher concentrations of dissolved Mn were found mainly in the shelf regions (> 10 nM) while low levels of dissolved Mn were found in the shelf break (< 5 nM). Dissolved Mn concentrations in the ECS were higher in summer than in other seasons. There was no significant difference in the distribution of dissolved Mn in spring and autumn except for nearshore areas with special inputs (t-test, P < 0.05). Only a small number of stations had higher concentrations in the bottom layer during spring and autumn, which may be a result of the re-suspension of bottom sediments. It is worth noting that the distribution of dissolved Mn in the ECS changed significantly in summer. Dissolved Mn concentration were at their maximum (up to 81.5 nM) in the near-bottom low-oxygen region in the coastal area adjacent to the Changjiang Estuary.

## 3.3 Vertical distribution of dissolved Mn in the East China Sea

Data obtained from the deep waters of section KW (Figure 1A, D12→D10→C14→C12) during the summer cruise were used to investigate the vertical distribution of dissolved Mn in the ECS (Figure 6). The KSW, KSSW, and KIW can be clearly distinguished from one another. The highest salinity water (> 34.5) occurred in the KSSW between 50 and 400 m. Vertical profiles of dissolved Mn in the KW generally exhibited a surface maximum, a mid-depth minimum in the KSSW, and a gradual increase near the bottom. These results indicated that the vertical distribution of dissolved manganese in the out shelf of the ECS presents a characteristic of surface enrichment and depletion at depth. The concentrations of dissolved Mn in the KSW ranged from 3.4 to 6.5 nM while it remained at relatively lower concentrations in the KSSW (< 2 nM). Interestingly, the concentration of dissolved Mn in the KSW was much higher at St. C14 than St. D12, which had relatively low salinity (33.7-34.0).
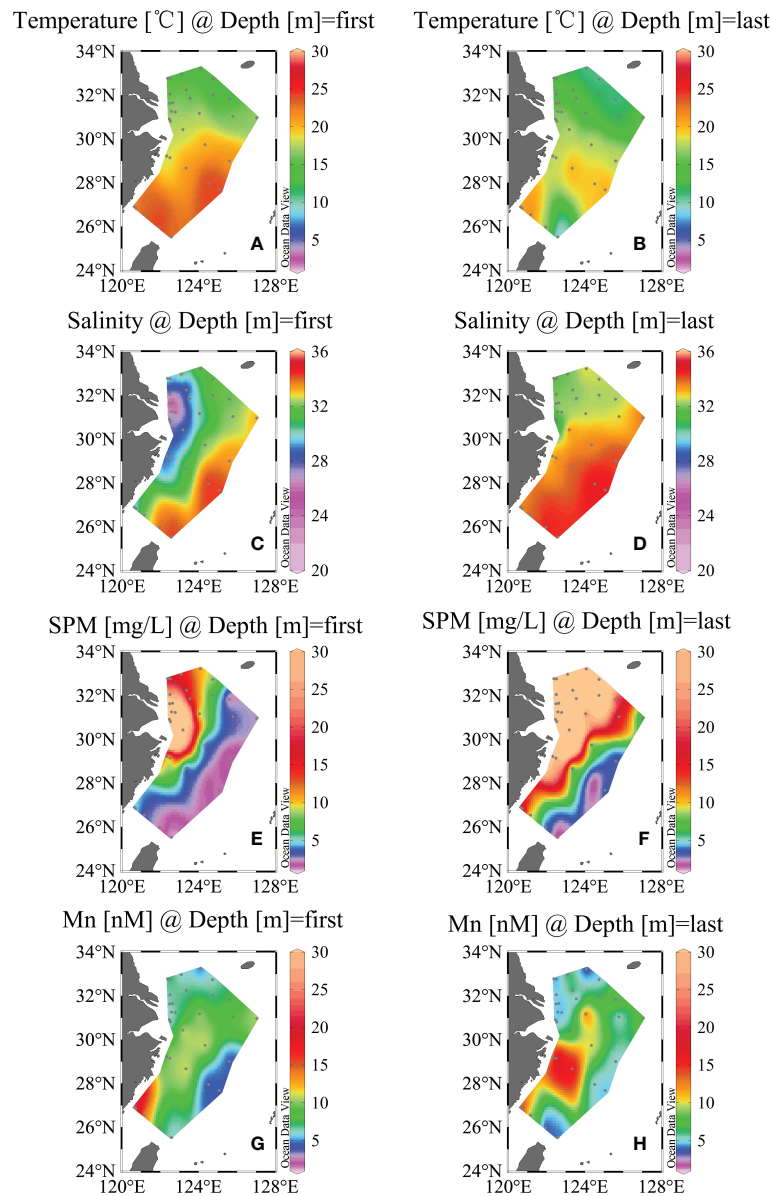
**FIGURE 3**

Horizontal distributions of temperature (°C), salinity, SPM (mg/L), and dissolved Mn (nM) in the surface **(A, C, E, G)** and the bottom layers **(B, D, F, H)** in the East China Sea in May 2013.

# 4 Discussion

## 4.1 Seasonal variations of dissolved Mn in ECS and its level in marginal seas

Although the biogeochemical cycle of dissolved Mn in the open ocean has been studied for more than half a century, relatively little research had been done in the marginal seas, especially in China. By conducting 3 cruises at different seasons, we aim to address seasonal variations of dissolved Mn in the ECS. The highest concentrations of dissolved Mn occurred in summer, while the range and average concentration in spring and autumn were almost the same (Figure 7). In spring and autumn, the concentration of dissolved Mn was slightly higher in surface waters than in the bottom waters, presumably because of the freshwater input and/or dust input (Tan

et al., 2012). In summer, the concentration of dissolved Mn was significantly higher in the bottom waters than in the surface waters ($t$-test, $P < 0.05$). Large increases of dissolved Mn in bottom waters in summer were associated with the onset of hypoxia in ECS (Wang et al., 2016). Inter-annual variations of dissolved Mn in the ECS are not easily noticeable. Interesting features revealed that dissolved Mn undergoes significant seasonal variations in the ECS, and that changes in the redox environment played an important role in controlling the source of dissolved Mn.

Comparisons of dissolved Mn among the ECS and other global marginal seas are shown in Table 2. Since dissolved Mn is highly influenced by regional environmental differences, the concentration ranges of dissolved Mn differ greatly among marginal seas. For example, in the anoxic environments of the Black Sea, Baltic Sea, and the Dead Sea, the dissolved Mn concentration is maintained at a
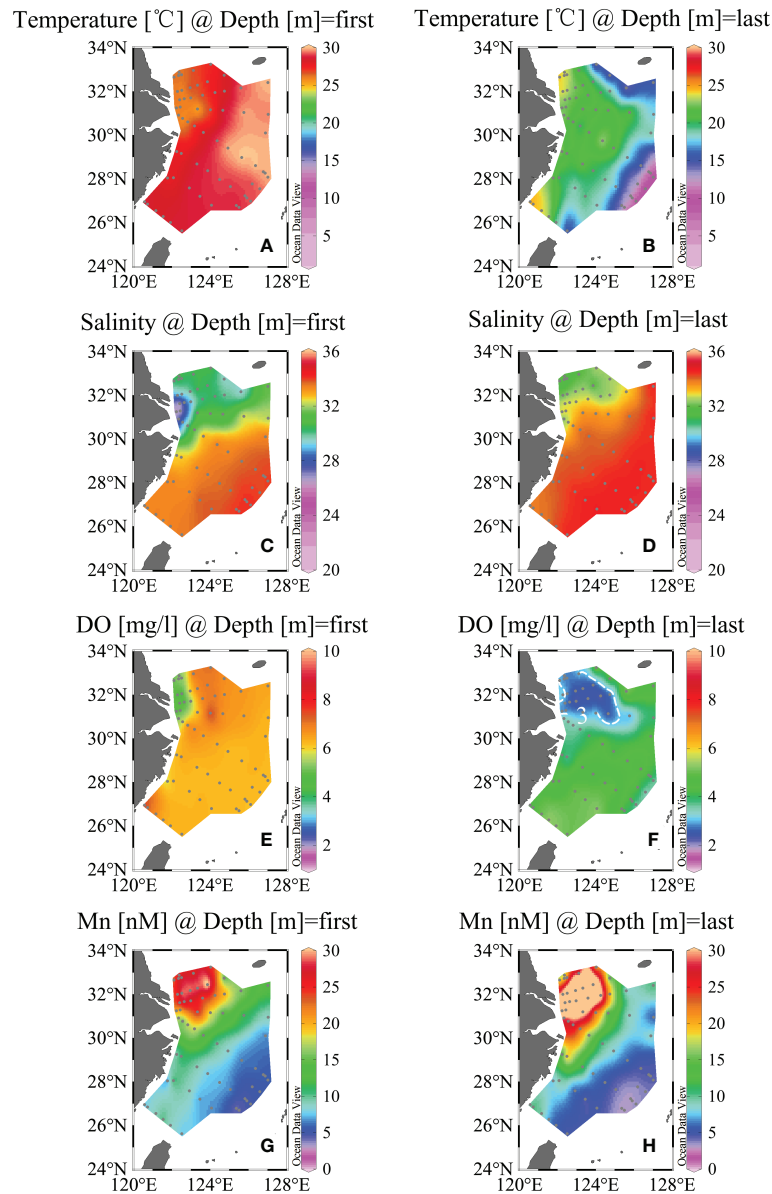
**FIGURE 4**
Horizontal distributions of temperature (°C), salinity, dissolved oxygen (DO, mg/L), and dissolved Mn (nM) in the surface **(A, C, E, G)** and the bottom layers **(B, D, F, H)** in the East China Sea in August 2013.

high level (μM rather than nM), especially in the oxygen minimum zone (OMZ) (Table 1). Elevated concentrations of dissolved Mn in water bodies have consistently been found under low oxygen conditions (if oxygen drops below 120 mM, Lewis and Luther, 2000; Yemenicioglu et al., 2006; Yakushev et al., 2009), which may be due to reduction of Mn oxides and degradation of organic materials (Wang et al., 2016). Marginal seas receiving large inputs from land runoff, such as the East China Sea, South China Sea, Columbia Estuary, and Coastal Red Sea also have high dissolved Mn concentrations (usually dozens of nM). However, in relatively open areas such as the Weddell Sea, Philippine Sea, and the Sargasso Sea the concentration of dissolved Mn is quite low (below 1 nM, although the surface layer can reach 4–5 nM) because they are far from land and receive little terrestrial input. Using previously reported data we can estimate that the world average dissolved Mn concentration in

marginal seas ranges from 7–38 nM and that dissolved Mn has a relatively short residence time ranging from 5–19 yr (Jickells, 1999; de Jong et al., 2007).

## 4.2 Processes controlling the distribution of dissolved Mn in the ECS

The behavior of dissolved Mn acts as a sensitive proxy for different terrestrial input and redox cycling in marine environments. The major source and space-time variations of dissolved Mn in the ECS are relatively complex. This study may be helpful to deepen understanding of these issues in the marginal seas.

*Water masses mixing*: Changjiang serves as the main source of terrestrial materials for the ECS as it supplies over 90% of the total
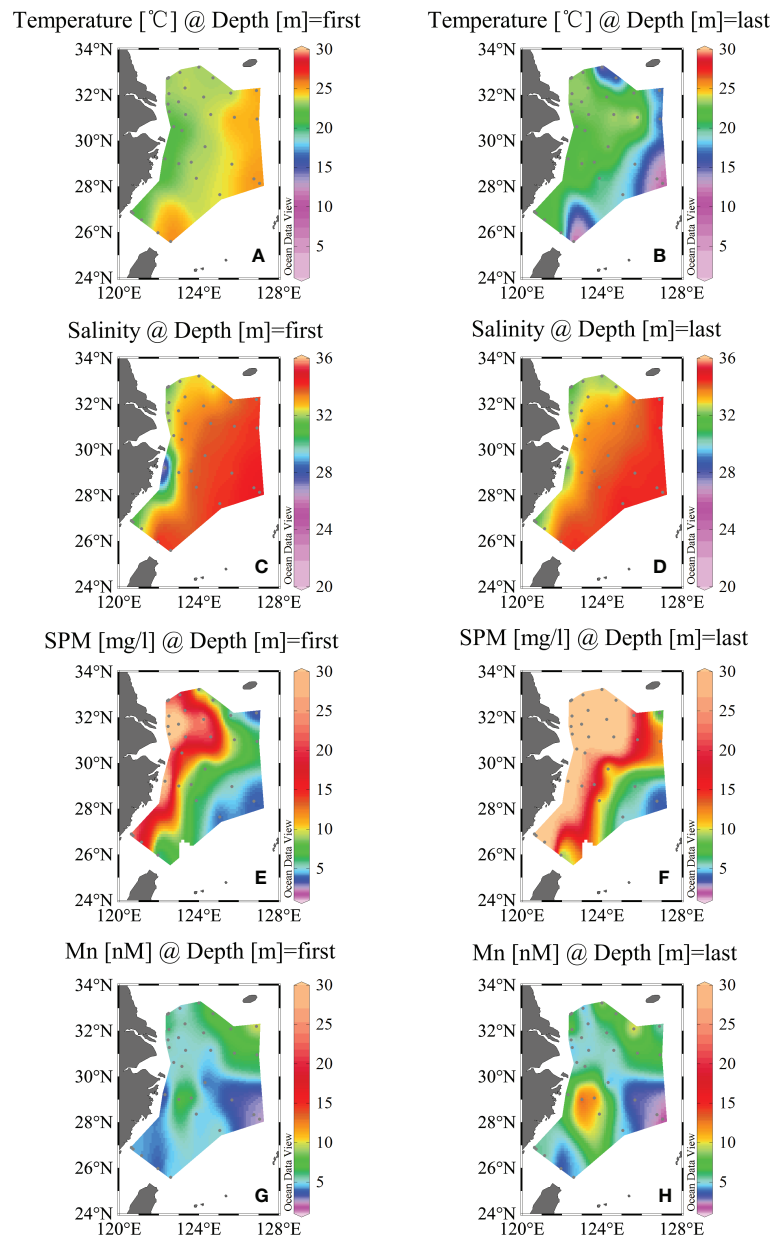
FIGURE 5
Horizontal distributions of temperature (°C), salinity, SPM (mg/L), and dissolved Mn (nM) in the surface **(A, C, E, G)** and the bottom layers **(B, D, F, H)** in the East China Sea in October 2013.

discharge of freshwater (Zhang et al., 2007). All samples during these cruises were divided into four subareas based on geographic locations (Figure 8): samples in the Changjiang plume, which show the Changjiang input into the ECS; samples in the inner shelf (depth < 50 m), which was strongly influenced by terrestrial/bottom boundary inputs; samples in the outer shelf (50 m < depth < 200 m), which was influenced by different water masses mixing; and samples in the Kuroshio mainstream water (depth > 200 m). The average concentrations of dissolved Mn in the Changjiang plume, inner shelf, outer shelf, and Kuroshio were (32.9 ± 25 nM), (15.4 ± 20 nM), (6.4 ± 2 nM) and (3.1 ± 1 nM), respectively. The highest concentrations of dissolved Mn were found in the Changjiang plume. The gradual decrease of dissolved Mn with distance reflects the contribution from the terrestrial input (Wang et al., 2016). The PN section from the

Changjiang Estuary to the Ryukyu Islands crosses the whole ECS continental shelf to Kuroshio (Figure 1), and it has become one of the most representative sections to study the distribution of dissolved metals under the effect of water masses mixing. We compared the vertical profiles of dissolved Mn in the PN section at different seasons (Figure 9). The Changjiang estuary (within 150 km of the Changjiang mouth in the PN section) has the highest concentration of dissolved Mn in summer affected by the CDW, followed by spring and the smallest in autumn, especially for the surface waters. Away from the Changjiang Estuary in relatively open waters, a low-Mn plume intruded into the ECS continental shelf, reflecting the influence of the KW (Yang et al., 2018). Seasonal variation of dissolved Mn in the PN section indicates that mixing of different water masses plays an important role in redistribution of dissolved Mn in the ECS.
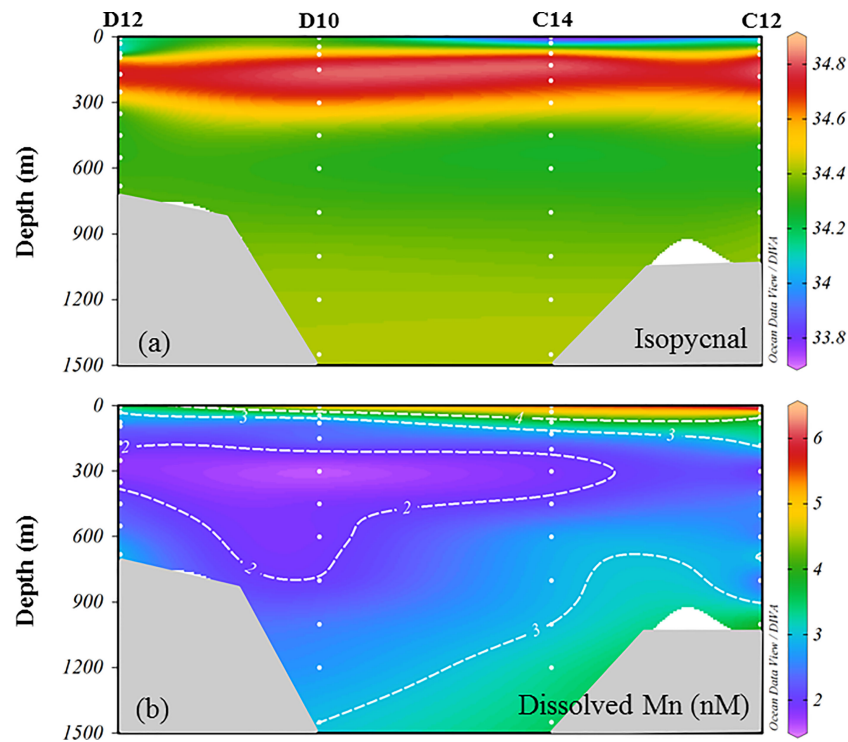
**FIGURE 6**
Vertical distributions of salinity **(A)** and dissolved Mn **(B)** across the KW section.

*Redox cycling*: Increasing concern has recently developed regarding hypoxia in the Changjiang Estuary (Zhu et al., 2016). Mn is a redox-sensitive element. The behavior of dissolved Mn in the Changjiang Estuary needs to be considered if the redox environment changes. We first compared vertical profiles of dissolved oxygen (DO) and dissolved Mn at *st.* N4 (123.4°E, 32.2°N) in different seasons (Figure 10A). In May, the concentration of dissolved Mn at *st.* N4 was less than 10 nM. In August, it increased to more than 60 nM in near-bottom waters experiencing hypoxia (DO < 3 mg/L). By October, the dissolved Mn concentration had returned to the level seen in May. Organic matter decomposition plays an important role in the process of oxygen depletion in the Changjiang Estuary. Data on the ratio of dissolved organic nitrogen and dissolved inorganic nitrogen (DON/DIN) is used here as a simple proxy to indicate the degree of the organic matter decomposition processes. The lower the ratio of DON/DIN, the higher the degree of organic matter decomposition (Zhu et al., 2016). The near-bottom data of apparent oxygen utilization (AOU), nutrients data of DON/DIN, and dissolved Mn were used to further investigate the internal mechanism of regeneration of dissolved Mn under hypoxia conditions (Figures 10B, C). Dissolved Mn concentration was positively correlated with the bottom AOU ($r$ = 0.72, n = 24), indicating that the regeneration of dissolved Mn is related to the degree of oxygen consumption. Dissolved Mn is negatively correlated with DON/DIN, which confirms that the high value of dissolved Mn is largely caused by organic matter decomposition in the hypoxic zone. We can conclude that dissolved Mn in near-bottom waters is substantially controlled by the redox environment in summer, and the form of Mn in seawaters changes rapidly in reduction environments.

*Shelf export*: The ECS continental shelf continues to receive terrestrial inputs (Changjiang) and shelf benthic inputs, causing the continental shelf to be rich in terrigenous materials. The off-shelf transport of terrestrial materials from continental shelf waters to out shelf waters in the ECS is recognized as one of the important processes for the biogeochemical cycle of biogenic elements (Yool and Fasham, 2001; Ya et al., 2017). The KW is an important carrier for receiving those terrestrial materials from the ECS continental shelf. An important clue to this lateral transportation of dissolved Mn in the ECS is that the vertical profiles of dissolved Mn in the KW varies significantly with different geographic locations and hydrographic regimes (Figure 11). It is noteworthy that the background concentration of dissolved Mn in KSW was approximately 1.0 nM. It increased to 3–4 nM at F8 and D12, then further increased to above 6 nM at St. C12 as the KW flows across the ECS shelf edge. Those signals can be ignored in deep waters. The enrichment of dissolved Mn in the KSW can be attributed to the off-shelf transport of Mn-rich continental shelf waters. Previous report also suggested that the influence of aerosol Mn inputs could not result in such a large increment of dissolved Mn in the KSW (Hsu et al., 2010; Jiang et al., 2018).

## 4.3 Quantitative estimation of exchange fluxes of dissolved Mn across the 100− and 200−m isobaths

Water exchange between the ECS continental shelf and the KW result in mesoscale dynamic processes, leading to both on-shelf and
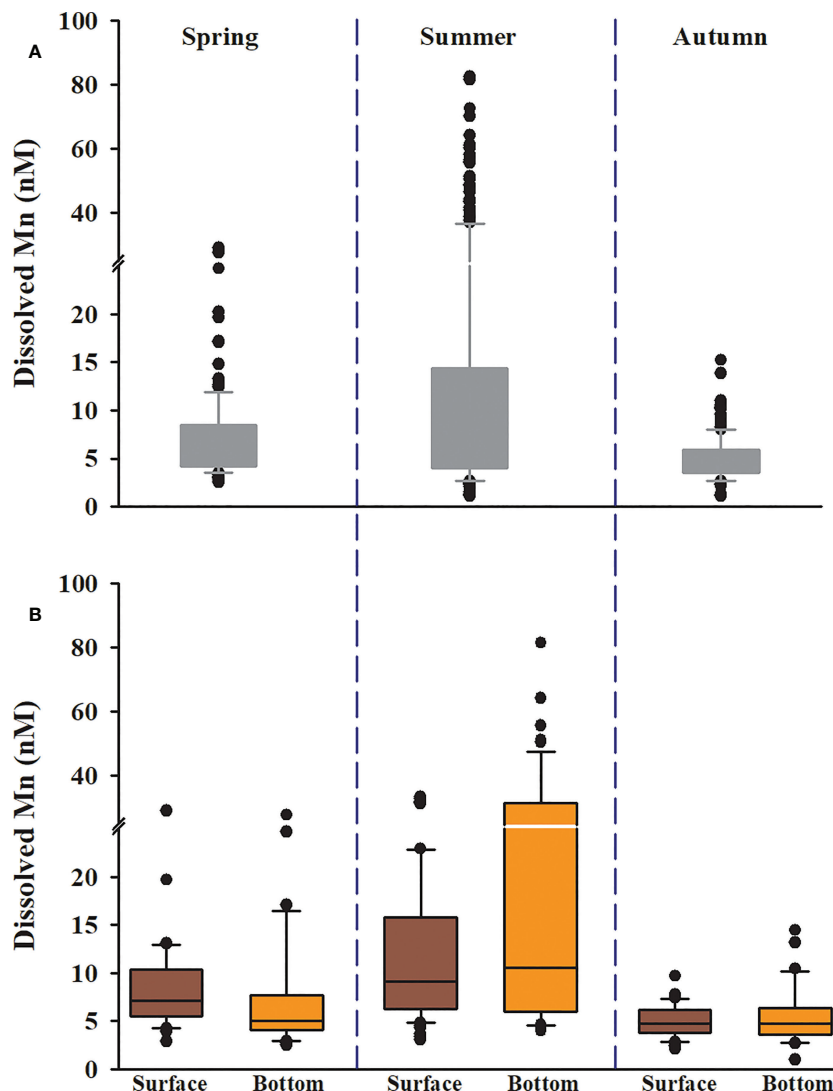
**FIGURE 7**
Statistical distribution of seasonal changes **(A)**, surface and bottom data **(B)** of dissolved Mn in the East China Sea.

**TABLE 1**  Comparison of dissolved manganese concentrations in ECS with global marginal seas.

| Region | Sampling time(year) | Mn concentration(nM) | Reference |
|---|---|---|---|
| East China Sea | 2013 | 1.1 – 20.5 | Present study |
| | | Hypoxia Zone: 9.1 – 81.5 | |
| | 2011 | 0.9 – 21.8 | Wang et al., 2016; Zhang et al., 2021b |
| | | Hypoxia Zone: 8.5 – 140.7 | |
| South China Sea | 2011, 2015 | 0.5 – 29.9 | Wang et al., 2018 |
| Weddell Sea | 2008 | ≤ 0.2 – 1.5 | Middag et al., 2013 |
| Baltic Sea | 2008 | > 1000 | Yakushev et al., 2009 |
| Philippine Sea | 2002 | < 0.4 – 4.5 | Obata et al., 2007 |
| Wadden Sea | 2002–2003 | 60 – 700 | Dellwig et al., 2007 |
| Black Sea | 2001 | > 1000 | Yemenicioglu et al., 2006 |
| | | | *(Continued)* |

**TABLE 1** Continued

| Region | Sampling time(year) | Mn concentration(nM) | Reference |
|---|---|---|---|
| Arabian Sea | 1995 | ≤ 0.6 – 8 | Lewis and Luther, 2000 |
| Columbia Estuary | 1994 | 12–40 | Klinkhammer et al., 1997 |
| Sargasso Sea | 1986 | 0.7 – 4.3 | Sunda and Huntsman, 1988 |
| Coastal Red Sea | 1980–1981 | 5.3 – 46 | Saad and Kandeel, 1988 |
| Dead Sea | 1977–1979 | > 1000 | Nishri, 1984 |

**TABLE 2** Fluxes of water and dissolved Mn across the 100−m isobath in the ECS (+: off−shelf, -: on−shelf).

| Region | Total Water Flux (Sv) | Total Mn Flux($\times 10^8$ mol/yr) | Depth (m) | Water Flux (Sv) | Mn concentration (nM) | Mn Flux($\times 10^8$ mol/yr) |
|---|---|---|---|---|---|---|
| A | −0.25 | −0.01 ± 0.20 | 0–10 | 0.12 | 4.4 ± 0.9 | 0.17 ± 0.03 |
|   |   |   | 10–65 | 0.23 | 3.1 ± 0.8 | 0.22 ± 0.06 |
|   |   |   | 65–100 | −0.60 | 2.1 ± 0.6 | −0.40 ± 0.11 |
| B | 1.14 | 1.52 ± 0.17 | 0–10 | 0.18 | 6.5 ± 1.1 | 0.37 ± 0.06 |
|   |   |   | 10–65 | 0.71 | 4.1 ± 0.4 | 0.92 ± 0.09 |
|   |   |   | 65–100 | 0.25 | 2.9 ± 0.3 | 0.23 ± 0.02 |
| C | −0.15 | −0.02 ± 0.08 | 0–10 | 0.08 | 3.8 ± 1.1 | 0.10 ± 0.03 |
|   |   |   | 10–65 | 0.05 | 3.7 ± 0.8 | 0.06 ± 0.01 |
|   |   |   | 65–100 | −0.28 | 2.1 ± 0.4 | −0.18 ± 0.04 |
| D | 1.39 | 3.06 ± 0.48 | 0–10 | 0.25 | 8.2 ± 1.3 | 0.65 ± 0.10 |
|   |   |   | 10–65 | 0.90 | 6.8 ± 1.1 | 1.93 ± 0.31 |
|   |   |   | 65–100 | 0.24 | 6.1 ± 0.9 | 0.48 ± 0.07 |
| E | 0.73 | 1.14 ± 0.21 | 0–10 | 0.25 | 5.2 ± 1.0 | 0.41 ± 0.08 |
|   |   |   | 10–65 | 0.66 | 4.2 ± 0.5 | 0.87 ± 0.10 |
|   |   |   | 65–100 | −0.18 | 2.4 ± 0.6 | −0.14 ± 0.03 |
| Total | 2.86 | 5.69 ± 1.14 |   |   |   |   |
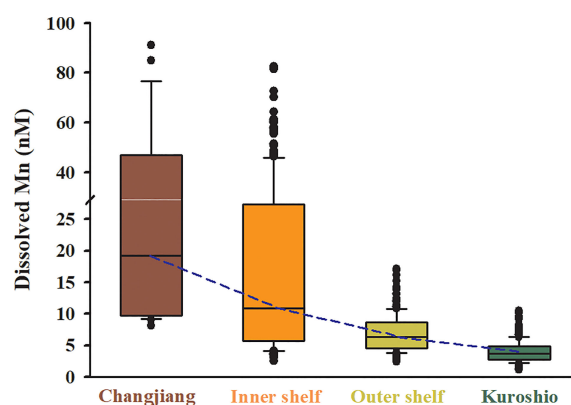


**FIGURE 8**

Dissolved Mn concentration distribution throughout the East China Sea. All samples were divided into four groups: the Changjiang plume, Inner shelf, Outer shelf, and Kuroshio waters.
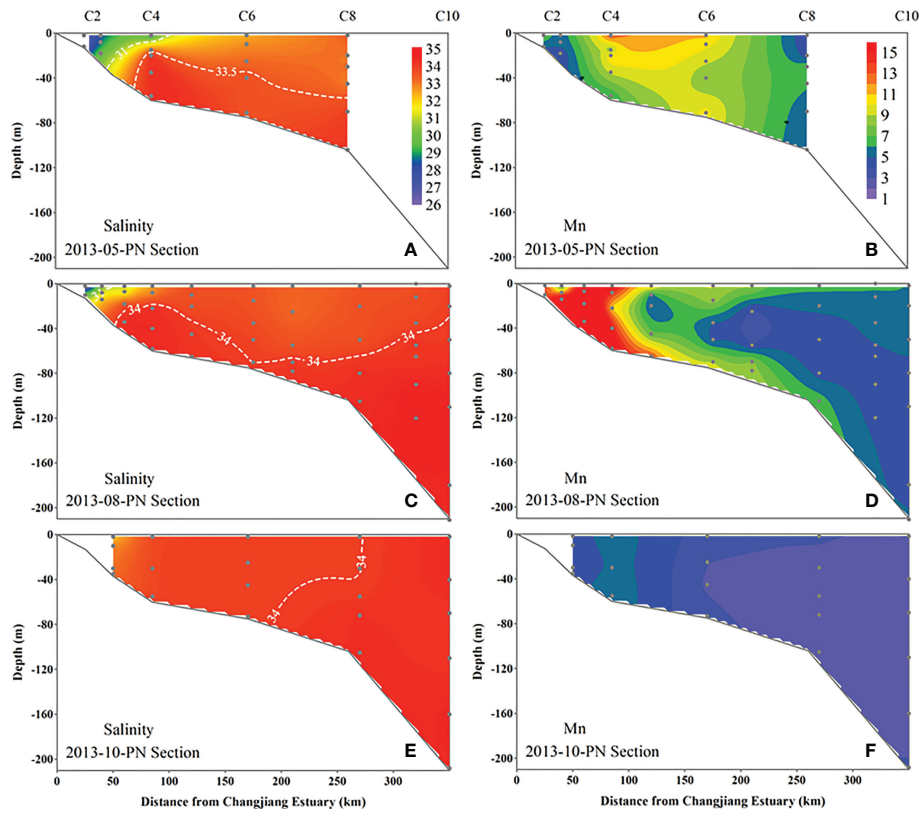
**FIGURE 9**
Seasonal variations of salinity **(A, C ,E)** and dissolved Mn (nM, **B ,D, F)** (nM) across the PN section.
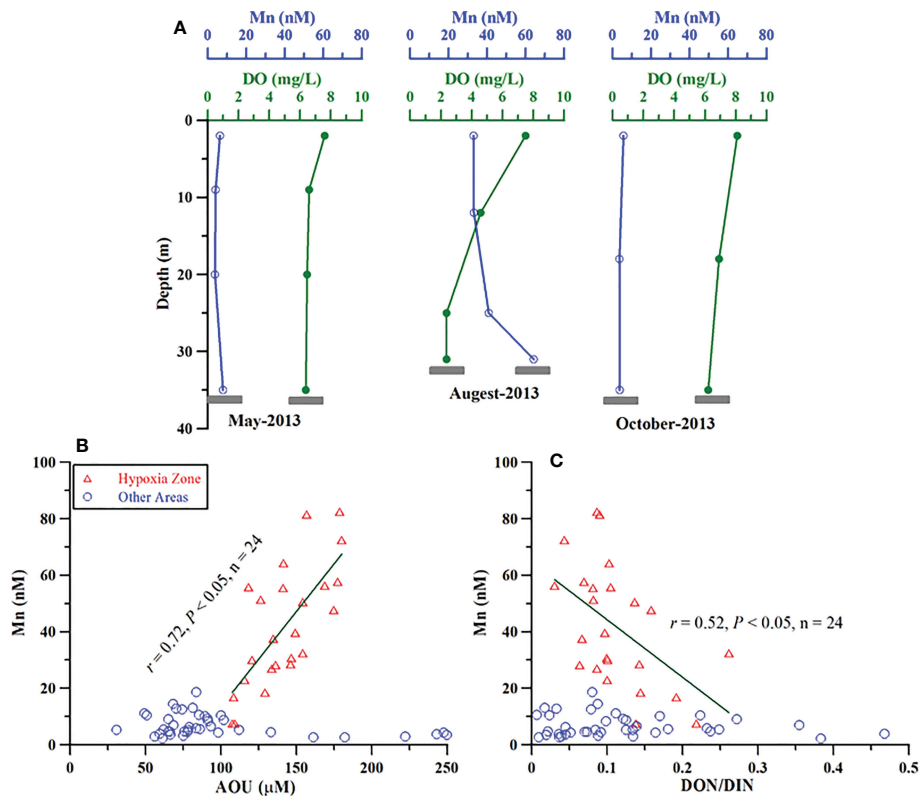


**FIGURE 10**
Comparison of seasonal profiles of dissolved oxygen and dissolved Mn at station N4 in the Changjiang Estuary **(A)**. Bottom dissolved Mn concentration plotted as a function of AOU **(B)** and DON/DIN **(C)**. The hypoxic zone is emphasized with a red triangle.
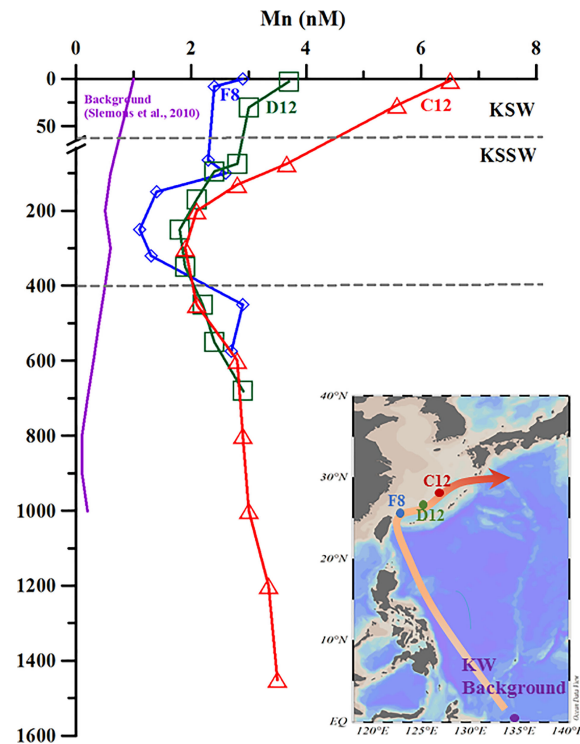
**FIGURE 11**
Vertical profiles of dissolved Mn at stations F8, D12, and C12 along the Kuroshio flow through the ECS edge. The positions of the stations are marked on the map. The background data of dissolved Mn in the KW is cited from (Slemons et al., 2010).

off-shelf transport (Guo et al., 2006; Zhou et al., 2015; Che and Zhang, 2018). This dynamic exchange driven by the physical mixing process not only modifies the properties of water masses but also pumps dissolved Mn transport in the ECS, which is recognized as an important issue for quantifying biogeochemical cycling in the ocean (Guo et al., 2012). To further confirm the dynamic variation of water and dissolved Mn exchanges across the ECS, the 100– and 200–m isobaths were selected as boundaries between the ECS continental shelf and the KW. We compared vertical distributions of current velocity and dissolved Mn at each grid point along the 100– and 200–m isobaths (Figure 12). The dynamic variations of on–shelf and off–shelf water exchanges across the 100– and 200–m isobaths were significant (t-test, P < 0.05). The KW with low concentrations of dissolved Mn intruded into the ECS continental shelf from the northeast of Taiwan, and the on–shelf intrusion of KW water across the 100–m isobath occurred at 27.2°N, 122.7°E (between grid numbers 30 and 60, Figure 2). The off-shelf transport of ECS continental shelf water across the 100–m isobath occurred at 28°N, 124°E (between grid numbers 60 and 80), and 30°N, 127°E (between grid numbers 150 and 170). The results fitted our prediction of lateral transport of dissolved Mn due to water masses mixing, and that the location of high concentrations of dissolved Mn is consistent with the off-shelf flow fields. A similar phenomenon can be found across the 100– and 200–m isobaths. Off–shelf transport of dissolved Mn across the 100–m isobath is more significant than across the 200–m isobath. The cross-shelf transport pattern in the ECS has also been well-validated by observational studies and numerical models (Ding et al., 2019; Zhang et al., 2019; Wang et al., 2021).

The exchange fluxes of dissolved Mn can be defined as the product of volume transport of water and representative Mn concentrations. The 100– and 200–m isobaths were divided into five horizontal sections based on flow direction and intensity (Figure 2). Each section was also divided into three layers based on the seawater density ($\sigma_\theta$; kg/m³, Wang et al., 2021): the upper layer ($\sigma_\theta < 21.5$), the middle layer ($21.5 < \sigma_\theta < 24.5$), and the deep layer ($\sigma_\theta > 24.5$). We used the average concentrations of dissolved Mn at ~5–10 km around each section across the 100– and 200–m isobaths as the representative concentrations of inflow and outflow transport to calculate the on–shelf and off–shelf fluxes of dissolved Mn, respectively. Details of the exchange fluxes of dissolved Mn across the 100– and 200–m isobaths are provided in Tables 2, 3. The ECS continental shelf is a net source of dissolved Mn for the adjacent waters. The net dissolved Mn transport flux across the 100– and 200–m isobaths is $(5.69 \pm 1.14) \times 10^8$ mol/yr and $(1.02 \pm 3.12) \times 10^8$ mol/yr, respectively. The difference in dissolved Mn flux between the 100– and 200–m isobaths $[(4.67 \pm 4.26) \times 10^8$ mol/yr] indicates that most of the dissolved Mn from the ECS continental shelf is transported north to the East/Japan Sea through the Tsushima Strait. The dissolved Mn flux across the 200–m isobath enters into the KW $[(1.02 \pm 3.12) \times 10^8$ mol/yr], which could potentially affect the distribution of dissolved Mn in the Northwest Pacific. The contribution of off-shelf transport of dissolved Mn in the ECS obtained here is comparable to previously published results for dissolved aluminum and neodymium (Ren et al., 2015; Che and Zhang, 2018). These results indicate the important contribution of cross-shelf transport to the geographical distribution of biogenic elements and their biogeochemical cycles in marginal seas.
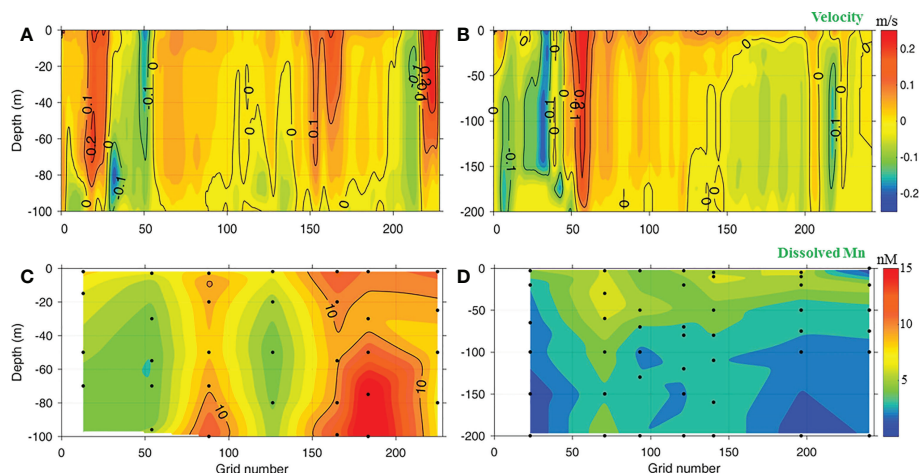
**FIGURE 12**
Current velocity distributions (m/s, **A, B**) and dissolved Mn distributions (nM, **C, D**) along the 100− and 200−m isobaths originating from Taiwan (+: off−shelf, −: on−shelf). Grid numbers represent locations used for the water budget calculation along the 100− and 200−m isobaths. Detailed information can be found in Figure 2. Part of the dissolved Mn data (Grid number > 180) comes from unpublished data from other cruises.

# 5 Summary and conclusions

In this study, we investigated the distribution of dissolved Mn in the ECS on three cruises in various seasons. There was a clear seasonality in dissolved Mn concentrations in the ECS, with the highest concentrations occurring in summer. The internal biogeochemical cycle of dissolved Mn in the ECS was influenced by a combination of Changjiang input, redox cycling, water masses mixing and cross-shelf transport. We demonstrated that the waters adjacent to the ECS receive a significant amount of Mn through

cross−shelf transport processes. This off−shelf transport flux of dissolved Mn across the 100− and 200−m isobaths through the ECS continental shelf was further quantitatively estimated. The total Mn export from the ECS continental shelf was $(5.69 \pm 1.14) \times 10^8$ mol/yr across the 100−m isobath. Nearly 82% of the total output enters into the East/Japan Sea, while the remaining 18% enters into the Kuroshio current. Our findings contribute to a better understanding of the behaviors influencing Mn biogeochemical cycles as well as defining the role of cross−shelf transport processes in the ECS. Future research needs to be focused on the physical mechanisms controlling shelf

**TABLE 3** Fluxes of water and dissolved Mn across the 200−m isobath in the ECS (+: off−shelf, -: on−shelf).

| Region | Total Water Flux (Sv) | Total Mn Flux(× $10^8$ mol/yr) | Depth (m) | Water Flux (Sv) | Mn concentration (nM) | Mn Flux(× $10^8$ mol/yr) |
|---|---|---|---|---|---|---|
| A' | −3.19 | −2.56 ± 0.80 | 0–65 | −1.12 | 3.5 ± 1.1 | −1.23 ± 0.39 |
|  |  |  | 65–100 | −1.36 | 2.1 ± 0.7 | −0.90 ± 0.30 |
|  |  |  | 100–200 | −0.71 | 1.9 ± 0.5 | −0.43 ± 0.11 |
| B' | 3.03 | 4.77 ± 1.27 | 0–65 | 1.77 | 5.8 ± 1.5 | 3.24 ± 0.84 |
|  |  |  | 65–100 | 0.96 | 4.2 ± 1.2 | 1.27 ± 0.36 |
|  |  |  | 100–200 | 0.30 | 2.7 ± 0.7 | 0.26 ± 0.07 |
| C' | 1.26 | 1.90 ± 0.43 | 0–65 | 1.00 | 5.2 ± 1.1 | 1.64 ± 0.35 |
|  |  |  | 65–100 | 0.22 | 3.3 ± 1.0 | 0.23 ± 0.07 |
|  |  |  | 100–200 | 0.04 | 2.4 ± 0.8 | 0.03 ± 0.01 |
| D' | −1.85 | −2.02 ± 0.46 | 0–65 | −0.46 | 4.9 ± 1.7 | −0.71 ± 0.25 |
|  |  |  | 65–100 | −0.79 | 3.4 ± 0.5 | −0.84 ± 0.12 |
|  |  |  | 100–200 | −0.60 | 2.5 ± 0.5 | −0.47 ± 0.09 |
| E' | −0.85 | −1.07 ± 0.16 | 0–65 | −0.22 | 5.4 ± 1.2 | −0.37 ± 0.08 |
|  |  |  | 65–100 | −0.29 | 4.7 ± 0.6 | −0.42 ± 0.05 |
|  |  |  | 100–200 | −0.34 | 2.6 ± 0.3 | −0.28 ± 0.03 |
| Total | −1.60 | 1.02 ± 3.12 |  |  |  |  |

transport and migration behavior through field observations and numerical simulations, as well as the significant contribution of using dissolved Mn as a tracer to track the output of terrestrial pollutants such as nutrients in the ocean.

## Conflict of interest

The authors declare that the research was conducted in the absence of any commercial or financial relationships that could be construed as a potential conflict of interest.

## Publisher's note

All claims expressed in this article are solely those of the authors and do not necessarily represent those of their affiliated organizations, or those of the publisher, the editors and the reviewers. Any product that may be evaluated in this article, or claim that may be made by its manufacturer, is not guaranteed or endorsed by the publisher.

## Supplementary material

The Supplementary Material for this article can be found online at: https://www.frontiersin.org/articles/10.3389/fmars.2022.1110913/full#supplementary-material

## References

Aguilar-Islas, A. M., and Bruland, K. W. (2006). Dissolved manganese and silicic acid in the Columbia river plume: A major source to the California current and coastal waters off Washington and Oregon. *Mar. Chem.* 101 (3), 233–247. doi: 10.1016/j.marchem.2006.03.005

Che, H., and Zhang, J. (2018). Water mass analysis and end-member mixing contribution using coupled radiogenic Nd isotopes and Nd concentrations: interaction between marginal seas and the northwestern pacific. *Geophys. Res. Lett.* 45 (5), 2388–2395. doi: 10.1002/2017GL076978

Colombo, M., Jackson, S. L., Cullen, J. T., and Orians, K. J. (2020). Dissolved iron and manganese in the Canadian Arctic ocean: on the biogeochemical processes controlling their distributions. *Geochim. Cosmochim. Ac.* 227, 150–174. doi: 10.1016/j.gca.2020.03.012

de Jong, J., Boye, M., Gelado-Caballero, M. D., Timmermans, K. R., Veldhuis, M. J. W., Nolting, R. F., et al. (2007). Inputs of iron, manganese and aluminum to surface waters of the northeast Atlantic ocean and the European continental shelf. *Mar. Chem.* 107 (2), 120–142. doi: 10.1016/j.marchem.2007.05.007

Dellwig, O., Bosselmann, K., Kölsch, S., Hentscher, M., Hinrichs, J., Böttcher, M. E., et al. (2007). Sources and fate of manganese in a tidal basin of the German wadden Sea. *J. Sea. Res.* 57 (1), 1–18. doi: 10.1016/j.seares.2006.07.006

Ding, R. B., Huang, D. J., Xuan, J. L., Zhou, F., and Pohlmann, T. (2019). Temporal and spatial variations of cross-shelf nutrient exchange in the East China Sea, as estimated by satellite altimetry and *in situ* measurements. *J. Geophys. Res-Oceans.* 124 (2), 1331–1356. doi: 10.1029/2018JC014496

Guo, X. Y., Miyazawa, Y., and Yamagata, T. (2006). The kuroshio onshore intrusion along the shelf break of the East China Sea: The origin of the tsushima warm current. *J. Phys. Oceanogr.* 36 (12), 2205–2231. doi: 10.1175/JPO2976.1

Guo, X. Y., Zhu, X. H., Wu, Q. S., and Huang, D. J. (2012). The kuroshio nutrient stream and its temporal variation in the East China Sea. *J. Geophys. Res-Oceans.* 117 (C1), 01026. doi: 10.1029/2011JC007292

Heiser, U., Neumann, T., Scholten, J., and Stüben, D. (2001). Recycling of manganese from anoxic sediments in stagnant basins by seawater inflow: a study of surface sediments from the gotland basin, Baltic Sea. *Mar. Geol.* 177 (1), 151–166. doi: 10.1016/S0025-3227(01)00129-3

Hsu, S. C., Wong, G. T. F., Gong, G. C., Shiah, F. K., Huang, Y. T., Kao, S. J., et al. (2010). Sources, solubility, and dry deposition of aerosol trace elements over the East China Sea. *Mar. Chem.* 120 (1), 116–127. doi: 10.1016/j.marchem.2008.10.003

Jan, S., Wang, J., Chern, C. S., and Chao, S. Y. (2002). Seasonal variation of the circulation in the Taiwan strait. *J. Mar. Syst.* 35 (3), 249–268. doi: 10.1016/S0924-7963(02)00130-6

Jiang, S., Zhang, J., Zhang, R. F., Xue., Y., and Zheng, W. (2018). Dissolved lead in the East China Sea with implications for impacts of marginal seas on the open ocean through cross-shelf exchange. *J. Geophys. Res-Oceans.* 123 (8), 6004–6018. doi: 10.1029/2018JC013955

Jickells, T. D. (1999). The inputs of dust derived elements to the Sargasso Sea: A synthesis. *Mar. Chem.* 68 (1), 5–14. doi: 10.1016/S0304-4203(99)00061-4

Klinkhammer, G. P., Chin, C. S., Wilson, C., Rudnicki, M. D., and German, C. R. (1997). Distributions of dissolved manganese and fluorescent dissolved organic matter in the Columbia river estuary and plume as determined by *in situ* measurement. *Mar. Chem.* 56 (1-2), 1–14. doi: 10.1016/S0304-4203(96)00079-5

Landing, W. M., and Bruland, K. W. (1987). The contrasting biogeochemistry of iron and manganese in the pacific ocean. *Geochim. Cosmochim. Ac.* 51 (1), 29–43. doi: 10.1016/0016-7037(87)90004-4

Lewis, B. L., and Luther, G. W.III (2000). Processes controlling the distribution and cycling of manganese in the oxygen minimum zone of the Arabian Sea. *Deep-Sea. Res. Pt. II.* 47 (7), 1541–1561. doi: 10.1016/S0967-0645(99)00153-8

Liu, K. K. (2000). Cross-shelf and along-shelf nutrient fluxes derived from flow fields and chemical hydrography observed in the southern East China Sea off northern Taiwan. *Cont. Shelf Res.* 20 (4), 493–523. doi: 10.1016/S0278-4343(99)00083-7

Middag, R., De Baar, H. J. W., Klunder, M. B., and Laan, P. (2013). Fluxes of dissolved aluminum and manganese to the weddell Sea and indications for manganese co-limitation. *Limnol. Oceanogr.* 58 (1), 287–300. doi: 10.4319/lo.2013.58.1.0287

Middag, R., De Baar, H. J. W., Laan, P., Cai, P. H., and van Ooijen, J. C. (2011). Dissolved manganese in the Atlantic sector of the southern ocean. *Deep-Sea. Res. Pt. II.* 58 (25), 2661–2677. doi: 10.1016/j.dsr2.2010.10.043

Middag, R., Séférian, R., Conway, T. M., John, S. G., Bruland, K. W., and De Baar, H. J. W. (2015). Intercomparison of dissolved trace elements at the Bermuda Atlantic time series station. *Mar. Chem.* 177, 476–489. doi: 10.1016/j.marchem.2015.06.014

Nishri, A. (1984). The geochemistry of manganese in the dead Sea. *Earth Planet. Sc. Lett.* 71 (2), 415–426. doi: 10.1016/0012-821X(84)90107-9

Obata, H., Doi, T., Hongo, Y., Alibo, D. S., Minami, H., Kato, Y., et al. (2007). Manganese, cerium and iron in the sulu, celebes and Philippine seas. *Deep-Sea. Res. Pt. II.* 54 (1), 38–49. doi: 10.1016/j.dsr2.2006.09.004

Qi, J. F., Yin, B. S., Zhang, Q. L., Yang, D. Z., and Xu, Z. H. (2014). Analysis of seasonal variation of water masses in East China Sea. *Chin. J. Oceanol. Limn.* 32 (4), 958–971. doi: 10.1007/s00343-014-3269-1

Ren, J. L., Xuan, J. L., Wang, Z. W., Huang, D. J., and Zhang, J. (2015). Cross-shelf transport of terrestrial Al enhanced by the transition of northeasterly to southwesterly monsoon wind over the East China Sea. *J. Geophys. Res-Oceans.* 120 (7), 5054–5073. doi: 10.1002/2014JC010655

Resing, J. A., Sedwick, P. N., German, C. R., Jenkins, W. J., Moffett, J. W., Sohst, B. M., et al. (2015). Basin-scale transport of hydrothermal dissolved metals across the south pacific ocean. *Nature* 523 (7559), 200–203. doi: 10.1038/nature14577

Roy, M., McManus, J., Goñi, M. A., Chase, Z., Borgeld, J. C., Wheatcroft, R. A., et al. (2013). Reactive iron and manganese distributions in seabed sediments near small mountainous rivers off Oregon and California (USA). *Cont. Shelf Res.* 54, 67–79. doi: 10.1016/j.csr.2012.12.012

Saad, M. A. H., and Kandeel, M. M. (1988). Distribution of copper, iron and manganese in the coastal red Sea waters in front of Al-ghardaqa. *Proc. Indian Natn. Sci. Acad.* 54 (4), 642–652.

Saager, P. M., De Baar, H. J. W., and Burkill, P. H. (1989). Manganese and iron in Indian ocean waters. *Geochim. Cosmochim. Ac.* 53 (9), 2259–2267. doi: 10.1016/0016-7037(89)90348-7

Sherman, K., and Tang, Q. (1999). Large Marine ecosystems of the pacific rim [M]. *Blackwell Sci.* 57-101:57-60. doi: 10.1016/0016-7037(89)90348-7

Shiller, A. M. (1997). Dissolved trace elements in the Mississippi river: seasonal, interannual, and decadal variability. *Geochim. Cosmochim. Ac.* 61 (20), 4321–4330. doi: 10.1016/S0016-7037(97)00245-7

Sim, N., and Orians, K. J. (2019). Annual variability of dissolved manganese in northeast pacific along line-p: 2010–2013. *Mar. Chem.* 216, 103702. doi: 10.1016/j.marchem.2019.103702

Slemons, L. O., Murray, J. W., Resing, J., Paul, B., and Dutrieux, P. (2010). Western Pacific coastal sources of iron, manganese, and aluminum to the equatorial undercurrent. *Global Biogeochem. Cy.* 24 (3), 1–16. doi: 10.1029/2009GB003693

Su, J. L. (1998). Circulation dynamics of the China seas north of 18∘ n. *Sea.* 11, 483–505.

Sunda, W. G., and Huntsman, S. A. (1988). Effect of sunlight on redox cycles of manganese in the southwestern Sargasso Sea. *Deep-Sea. Res. Pt. I.* 35 (8), 1297–1317. doi: 10.1016/0198-0149(88)90084-2

Tan, S. C., Shi, G. Y., and Wang, H. (2012). Long-range transport of spring dust storms in inner Mongolia and impact on the China seas. *Atmos. Environ.* 46, 299–308. doi: 10.1016/j.atmosenv.2011.09.058

Van Hulten, M. M. P., Dutay, J. C., Middag, R., De Baar, H. J. W., Roy-Barman, M., Gehlen, M., et al. (2016). Manganese in the world ocean: a first global model. *Biogeosci. Discussions.* 14 (5), 1123–1152. doi: 10.5194/bg-2016-282

Wang, Z. W., Ren, J. L., Jiang, S., Liu, S. M., Xuan, J. L., and Zhang, J. (2016). Geochemical behavior of dissolved manganese in the East China Sea: Seasonal variation,

estuarine removal, and regeneration under suboxic conditions. *Geochem. Geophy. Geosy.* 17 (2), 282–299. doi: 10.1002/2015GC006128

Wang, Z. W., Ren, J. L., Xuan, J. L., Li, F. M., Yang, T. T., and Guo, Y. (2018). Processes controlling the distribution and cycling of dissolved manganese in the northern south China Sea. *Mar. Chem.* 204, 152–162. doi: 10.1016/j.marchem.2018.07.003

Wang, Z. W., Xuan, J. L., Li, F. M., Ren, J. L., Huang, D. J., and Zhang, J. (2021). Monsoon-facilitated off-shelf tansport of dissolved aluminum across the East China Sea during summer. *J. Geophys. Res-Oceans.* 126 (6), 1–20. doi: 10.1029/2020JC016953

Wu, J. F., Roshan, S., and Chen, G. (2014). The distribution of dissolved manganese in the tropical–subtropical north Atlantic during US GEOTRACES 2010 and 2011 cruises. *Mar. Chem.* 166, 9–24. doi: 10.1016/j.marchem.2014.08.007

Xuan, J. L., Huang, D. J., Pohlmann, T., Su, J., Mayer, B., Ding, R. B., et al. (2017). Synoptic fluctuation of the Taiwan warm current in winter on the East China Sea shelf. *Ocean Sci.* 13 (1), 105–122. doi: 10.5194/os-13-105-2017

Xuan, J. L., Su, J., Wang, H., Huang, D. J., Ding, R. B., Zhou, F., et al. (2019). Improving low-resolution models *via* parameterisation of the effect of submesoscale vertical advection on temperature: A case study in the East China Sea. *Ocean Model.* 136, 51–65. doi: 10.1016/j.ocemod.2019.03.002

Xuan, J. L., Yang, Z. Q., Huang, D. J., Wang, T. P., and Zhou, F. (2016). Tidal residual current and its role in the mean flow on the changjiang bank. *J. Mar. Syst.* 154, 66–81. doi: 10.1016/j.jmarsys.2015.04.005

Yakushev, E., Pakhomova, S., Sørenson, K., and Skei, J. (2009). Importance of the different manganese species in the formation of water column redox zones: Observations and modeling. *Mar. Chem.* 117 (1), 59–70. doi: 10.1016/j.marchem.2009.09.007

Yang, S. C., Zhang, J., Sohrin, Y., and Ho, T. Y. (2018). Cadmium cycling in the water column of the kuroshio-oyashio extension region: Insights from dissolved and particulate isotopic composition. *Geochim. Cosmochim. Ac.* 233, 66–80. doi: 10.1016/j.gca.2018.05.001

Ya, M., Wang, X., Wu, Y., Li, Y., Yang, J., Fang, C., et al. (2017). Seasonal variation of terrigenous polycyclic aromatic hydrocarbons along the marginal seas of China: input, phase partitioning, and ocean-current transport. *Environ. Sci. Technol.* 51 (16), 9072–9079. doi: 10.1021/acs.est.7b02755

Yemenicioglu, S., Erdogan, S., and Tugrul, S. (2006). Distribution of dissolved forms of iron and manganese in the black Sea. *Deep-Sea. Res. Pt. II.* 53 (17), 1842–1855. doi: 10.1016/j.dsr2.2006.03.014

Yool, A., and Fasham, M. J. (2001). An examination of the "continental shelf pump" in an open ocean general circulation model. *Global Biogeochem. Cy.* 15 (4), 831–844. doi: 10.1029/2000GB001359

Zhang, J., Guo, X. Y., and Zhao, L. (2021a). Budget of riverine nitrogen over the East China Sea shelf. *Environ. pollut.* 289, 117915. doi: 10.1016/j.envpol.2021.117915

Zhang, K., Li, A., Huang, P., Lu, J., Liu, X., and Zhang, J. (2019). Sedimentary responses to the cross-shelf transport of terrigenous material on the East China Sea continental shelf. *Sediment. Geol.* 384, 50–59. doi: 10.1016/j.sedgeo.2019.03.006

Zhang, Y., Li, L., Ren, J. L., He, H. J., Zhang, R. F., Zhao, L., et al. (2021b). Distribution and influencing factors of dissolved manganese in the yellow Sea and the East China Sea. *Mar. Chem.* 234, 104002. doi: 10.1016/j.marchem.2021.104002

Zhang, J., Liu, S. M., Ren, J. L., Wu, Y., and Zhang, G. L. (2007). Nutrient gradients from the eutrophic changjiang (Yangtze river) estuary to the oligotrophic kuroshio waters and re-evaluation of budgets for the east china sea shelf. *Prog. Oceanogr.* 74 (4), 449–478. doi: 10.1016/j.pocean.2007.04.019

Zhang, R. F., Zhang, J., Ren, J. L., Li, J., Li, F. M., and Zhu, X. C. (2015). X-Vane: A sampling assembly combining a niskin-X bottle and titanium frame vane for trace metal analysis of sea water. *Mar. Chem.* 177, 653–661. doi: 10.1016/j.marchem.2015.10.006

Zheng, L., Minami, T., Konagaya, W., Chan, C. Y., Tsujisaka, M., Takano, S., et al. (2019). Distinct basin-scale-distributions of aluminum, manganese, cobalt, and lead in the north pacific ocean. *Geochim. Cosmochim. Ac.* 254, 102–121. doi: 10.1016/j.gca.2019.03.038

Zhou, F., Xue, H. J., Huang, D. J., Xuan, J. L., Ni, X. B., Xiu, P., et al. (2015). Cross-shelf exchange in the shelf of the East China Sea. *J. Geophys. Res-Oceans.* 120, 1545–1572. doi: 10.1002/2014JC010567

Zhu, J. R., Zhu, Z. Y., Lin, J., Wu, H., and Zhang, J. (2016). Distribution of hypoxia and pycnocline off the changjiang estuary, China. *J. Mar. Syst.* 154, 28–40. doi: 10.1016/j.jmarsys.2015.05.002